EXPERIMENTAL PROCESSING OF ULTRA-LOW CARBON STEEL USING VACUUM TREATMENT

*Hoang Le[1)], Cao-Son Nguyen[1)], Anh-Hoa Bui[1)]**
[1)] School of Materials Science and Engineering, Hanoi University of Science and Technology, Vietnam

Received: 16.12.2017
Accepted: 22.02.2018

**Corresponding author: hoa.buianh@hust.edu.vn, Tel.: 84-24-38680409; Department of Iron and Steelmaking, School of Materials Science and Engineering, Hanoi University of Science and Technology; No. 1, Dai Co Viet Road, Hai Ba Trung District, Hanoi, Vietnam*

Abstract
This paper presents experimental process of ultra-low carbon (ULC) steel using vacuum heat treatment. After adjusting the chemical compositions as desired, the ULC steel was casted into plate, hot-forged and cold-rolled to sheet of 1 mm thickness, finally annealed at 800°C. Microstructure, crystalline phase, non-metallic inclusions and mechanical properties of the ULC steels were characterized by optical microscopy, X-ray diffraction (XRD), energy-dispersive X-ray spectroscopy (EDS) and tensile test. Under argon vacuum atmosphere, decarburization occurred and C contents of the treated steels were reduced to 36 and 40 ppm corresponding to the decarburizing rate of 84.2 and 82.4%, respectively. The vacuum induction melting is thought to accelerate the rate of carbon removal from liquid steel. Electromagnetic force was attributed to promote the decarburization due to increasing the mass transfer coefficient during vacuum treatment. The annealed steels obtained a good combination of the strength and ductility; the total elongations were 45.2 and 42.9 %, while the yield strengths were 199 and 285 MPa, respectively. The results indicated that the ULC steels have only ferrite phase, of which grains size were 30 μm in average. The relative volume of non-metallic inclusions in the ULC steels was calculated as 0.23 vol. %, resulting positive contribution in the mechanical properties.

Keywords: ULC steel, vacuum heat treatment, carbon removal, microstructure, inclusions

1 Introduction

In production of ultra-low carbon (ULC) steel, efficiently removing carbon is an essential step which much affect quality and price of the final product; many attentions have thus focused on the carbon removal from liquid steel. When C content of liquid steel reaches to very low value, reaction between [C] and [O] hardly occurs in the normal pressure. The development of an effective method to decarburize during the secondary refining is desired. Before the appearance of vacuum treatment, lowest content of C was about 0.02% and the oxygen content reached 0.10% or more. It is possible to lower C content of less than 0.005% (≈ 50 ppm) using vacuum heat treatment of liquid steel, so the RH degasser is a potential process and provides a high productivity of ULC steel [1,2]. Decarburization in BOF occurs with a result that carbon can be reduced to minimum of 0.02-0.04 %, thereafter liquid steel is transferred to the RH treatment for continuously decarburizing. At such low C level, it is necessary to supply oxygen or/and create a vacuum atmosphere or/and increase turbulence of liquid steel in order to promote the rate of

DOI 10.12776/ams.v24i1.1070 p-ISSN 1335-1532
e-ISSN 1338-1156

decarburization. For example, RH-OB technology is a typical way of feeding the oxygen gas into the liquid steel during treatment. Since vacuum refining operates with high cost and complex equipment, the main interests have been focused on rate of C removal and morphology of non-metallic inclusion. J. Liu *et al.* reported that steelmaking companies needed to treat liquid steel within 10-25 minutes for reducing C content to 10-30 ppm [2]. M. Molnar *et al.* studied on the impact of chemical reheating on the cleanliness of heats processed at an vacuum degasser; then concluded that depending on a number of other process parameters, it could strongly affect the degree of steel cleanliness and casting conditions [3]. Another research was carried out to investigate inclusions in ULC steel melts consist mainly of Al oxides and multi-component oxide during an RH deoxidation treatment and confirmed that if these inclusions were not removed properly, they could deteriorate the properties of the final products [4].
Ladle degassing tank or vacuum suction degassing process is used for smaller production of ULC steel. In case of oxygen injection, excess oxygen can result in high oxygen content in the liquid steel after deep decarburization. This is undesirable because of a high consumption of deoxidizers and steel contamination with oxide inclusions. Since vacuum induction melting can be used in many applications owing to strong circulation, several efforts have mentioned on vacuum treatment of ULC steel using this technology [5-7]. Therefore, the present paper aims to experimentally processing ULC steel using vacuum treatment. Some characterizing methods were used to study on correlation of the mechanical properties and microstructures.

2 Experimental

Chemical compositions of the initial steel, which C content is similar to the liquid steel tapped from BOF to vacuum treatment in the practical, are listed in **Table 1**. Experimental vacuum treatment was conducted in a high frequency induction furnace (ALD) under argon vacuum pressure of 0.2 atm. An amount of the initial steel (0.5 kg) was contained in a magnesia crucible (ID ϕ40×70 mm), then melted and remained at 1600°C for 10 minutes. Thereafter, a given amount of high purity silicon (Si) and manganese (Mn) were added into the liquid steel to adjust the compositions as obtained in **Table 1**. The treated steel was casted into plate (40×25×20 mm) which was hot-forged to 10 mm thickness, then directly cold-rolled to sheets with several passes. The final cold reduction was controlled as 90 % with 1 mm thickness of the steel sheets. Cold-rolled sheets were annealed at 800°C for 15 minutes. Standard specimens (ASTM A370) of the cold-rolled and annealed steels were cut longitudinally the rolling direction and subjected to tensile testing using a MTS 809.10A machine. Microstructure of cross-section of the steels was observed using an optical microscope (Axiovert 25A). X-ray diffraction (XRD, Bruker) and electron probe micro-analysis (EPMA, JEOL) were used to characterize phase and non-metallic inclusions of the steel.

Table 1 Chemical compositions of the initial steel (% mass)

	Symbol	C	Mn	Si	P	S	Fe
Initial steel	TN2	0.0228	0.0146	0.0144	0.0193	0.0081	Balance
Treated steel	TN2-2	0.0036	0.1953	0.0354	0.0198	0.0088	Balance
	TN2-3	0.0040	0.4151	0.1748	0.0011	0.0082	Balance

3 Results and Discussion

Chemical compositions of the treated steel are given in **Table 1**. It was seen that decarburization of the liquid steel occurred during the vacuum treatment, so the C content was reduced to ultra-

DOI 10.12776/ams.v24i1.1070 p-ISSN 1335-1532
e-ISSN 1338-1156

low level. This can be explained that vacuum atmosphere above the liquid steel promoted the reaction (1), in which K_{CO} is the equilibrium constant. At 1600°C, it is acknowledged that $[C]\times[O] = 0.002\times P_{CO}$ [8]. When the C content of liquid steel is very low, the reaction (1) does not occur at the pressure of 1 atm, but can occur at vacuum atmosphere. The CO bubbles move out from the liquid steel easily, i.e. decarburization can continue at ultra-low carbon level. In term of kinetics, vacuum atmosphere did not improve the diffusion in the gaseous phase, but also increases the decarburizing rate [2,9]. The efficiency and the rate of vacuum decarburizing treatment were calculated as in **Table 2**, where the efficiency was 82.5-84.2% and the decarburizing rate was about 19 ppm per minute. It is known that the efficiency of vacuum decarburizing treatment depends on the initial C content, the processing duration and the vacuum level. In the present experiment, a strong stirring of the liquid steel caused by the magnetic force was attributed to the deep removal of carbon. Moreover, vacuum Ar atmosphere above the liquid steel was a factor that positively influenced on the decarburizing treatment [10,11].

$$[C] + [O] = \{CO\} \quad (1.)$$

$$\Delta G^{o} = -22200 - 38{,}34T\ (J.mol^{-1})\ ;\ K_{CO} = \frac{P_{CO}}{[C]\times[O]}$$

Table 2 Efficiency and rate of vacuum decarburizing treatment

Symbol	**[**ppm **C], initial**	**[**ppm **C], treated**	**Δ[** ppm **C] removal**	**Efficiency, %**	**The rate of decarburization, [**ppm **C]/min**
TN2-2	228	36	192	84.2	19
TN2-3	228	40	188	82.5	19

It is acknowledged changing the thermodynamic equilibrium with decreasing pressure is the principle for decarburization and degassing. The kinetics of thermo-chemical reactions is particularly relevant for an efficient process time. Decarburization is a complicated heterogeneous process consisting of several stages, each of which can theoretically control the overall reaction rate. M. A. Makarov *et al.* studied on equilibrium of the reaction (1) and concluded that deoxidizing capacity of C is inversely proportional to the gaseous phase pressure, i.e. a decrease in the pressure from 1 to 0.01 atm should be accompanied by an increase in the deoxidizing capacity of C by 10 and 100 times, respectively [10]. Since the gaseous nucleus has to overcome the forces of the surface tension and the ferrostatic pressure of the liquid metal column, the pressure of CO gas nucleus in the zone of interaction of [C] and [O] should considerably exceed P_{CO} in the gaseous phase above the liquid metal. M. Sano *et al.* concluded that C concentration could be decreased to a few ppm, the rate constant of decarburizing reaction in a vacuum atmosphere would follow the apparent first-order and the metal-phase mass transfer coefficient for an inductively stirred iron melt was about 0.02-0.04 cm/s depending on vacuum pressure above the liquid steel [5].

Table 3 Mechanical properties of the ULC steels

	Cold-rolled			Annealled		
	UTS (MPa)	YS (MPa)	EL (%)	UTS (MPa)	YS (MPa)	EL (%)
TN2-2	635	474	4.5	309	199	45.4
TN2-3	777	461	5.1	351	285	42.9

DOI 10.12776/ams.v24i1.1070 p-ISSN 1335-1532
e-ISSN 1338-1156

Mechanical properties including ultimate tensile strength (UTS), yield strength (YS) and elongation (EL) of the ULC steels are given in **Table 3**. It is seen that strengths of the ULC steel have been obtained good results despite of that the steels contained a small amount of strengthening elements such as Si and Mn. These alloying elements, which are usually added to compensate for the softening effect of ultra-low carbon content, contribute in the strengthening by solid solution hardening. Since the residual stress was not removed, the cold-rolled sheets were strengthened; and the UTS stayed in range of 635-777 MPa, the EL was low as 4.5-5.1 %. At the same condition, strengths of the steel TN2-2 were found to be lower than those of the steel TN2-3. In simplicity, this can be explained that lower content of Si and Mn in the ULC steel TN2-2 is the cause. However, the steel TN2-2 showed higher YS than the steel TN2-3. It is speculated that a severe cold-rolling (CR = 90 %) would have a negative effect on strengths of the steel TN2-3 which contained higher strengthening elements as Mn and Si. Therefore, a compromise between the compositions and the deformed condition of ULC steel needs to be concerned.

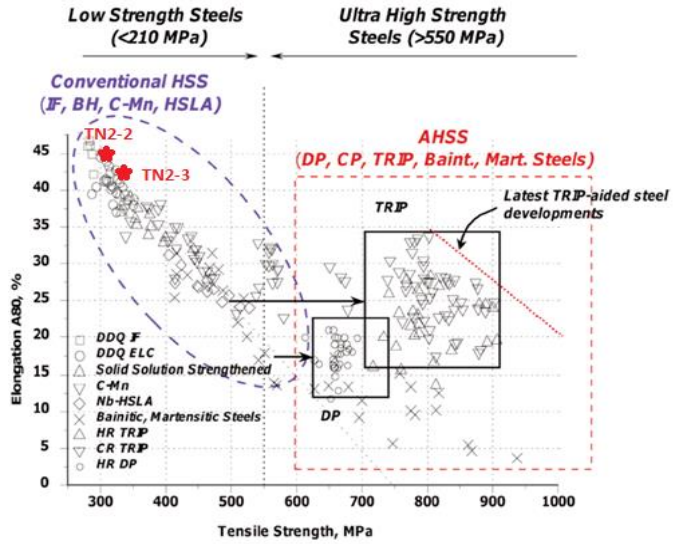

Fig. 1 Tensile strength versus elongation for various steels (after [12])

Although tensile ductility cannot be the criteria for the deep drawability of the steel, the total elongation should be the first evidence for evaluation because high ductility is usually associated with good quality during forming. In this study, the cold-rolled sheets, which shown a high strength and low elongation, were annealed to investigate improvement of the ductility. As the annealing temperature was 800ºC, the EL strongly increased to 42.9-45.4% while the YS decreased to 199-285 MPa. This result is in agreement with the automotive ULC steels which exhibit typically 200–280 MPa of YS and 30–47% of EL [1,13,14]. K. Dehghani *et al.* concluded that the YS of the steels should be as low as possible to avoid the aforementioned defects in press forming [15]. As far as the ULC steels are concerned, most research has been concerning on the formability improvement but keep high YS because this confers a high dent resistance for the steel. Thus, compromise between strength and ductility of the steel is essential to all producers. The relationship between tensile strength and elongation of the annealed ULC

DOI 10.12776/ams.v24i1.1070 p-ISSN 1335-1532
e-ISSN 1338-1156

steels (TN2-2 and TN2-3) is in comparison with other steels as shown in **Fig. 1**. Addition of suitable Mn and Si amount in the ULC steels has contributed positively in their mechanical properties. Mn is known as an important alloying element for solid solution strengthening, resulting improvement of the hardenability and the transformation of acicular ferrite which enhances of both strength and toughness of the steel [16,17]. Meanwhile, the addition of Si up to 0.6 wt% strengthens the ferrite matrix, but higher Si content has an adverse effect on the ductility of the steel [18].

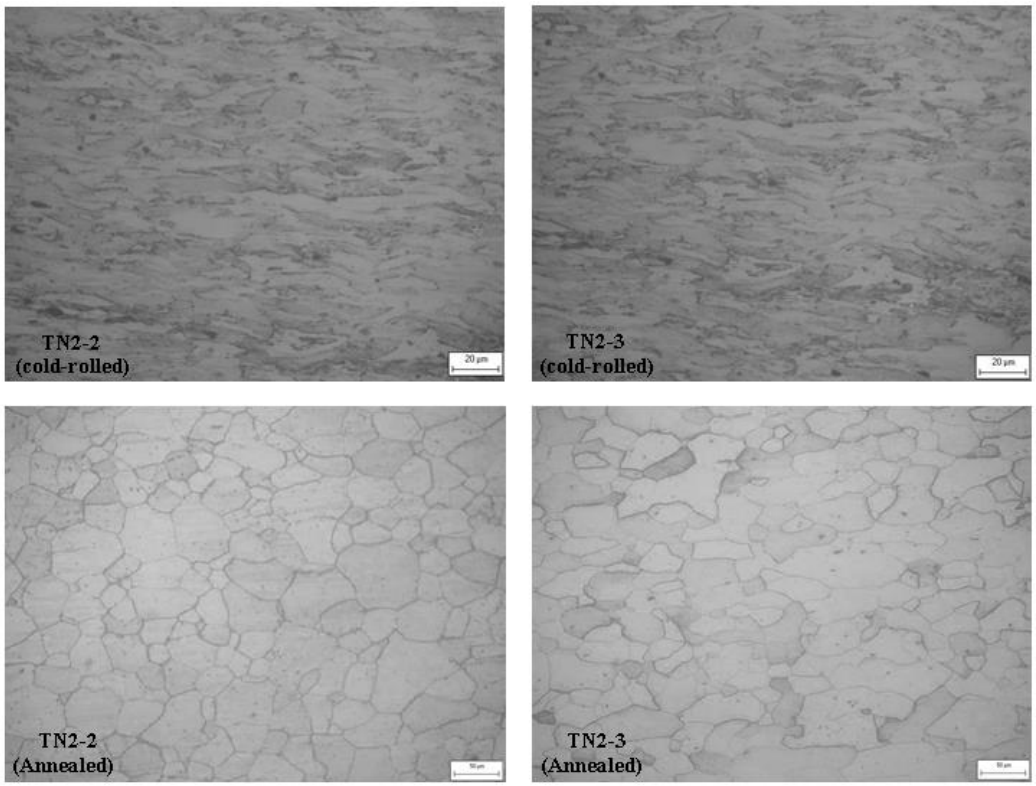

Fig. 2 Optical micrographs of the cold-rolled and annealed steel (TN2-2)

It can be confirmed that mechanical properties of the ULC steels is dependent on several factors as compositions, and the fact that a good combination of both the tensile properties and the ductility has been obtained after the steels annealed at 800°C. As similar to findings of Y. K. Lee *et al.*, the ferrite grains were coarsened at higher annealing temperature, consequently decreasing the strength and increasing the ductility of the steel sheets [19]. The stress relief and recrystallization was considered to be occurred at this annealing temperature. This can be asserted by microstructural observation of the annealed steel. **Fig. 2** shows typical micrographs of the cold-rolled and annealed steel, in which the cold-rolled microstructure was very homogeneous across the thickness; textures were found because the grains were deformed to lamina and elongated with the rolling direction. N. Yoshinaga *et al.* have carried out a study on effect of the deformed textures and microstructure on the subsequent recrystallization behavior of the IF steel, then remarks that the orientation distribution of the recrystallized grains forming

DOI 10.12776/ams.v24i1.1070 p-ISSN 1335-1532
e-ISSN 1338-1156

at the early stages of the recrystallization dominated the final microstructure [20]. It is clearly seen that the recrystallization occurred at annealing temperature of 800°C, at which various thermally activated processes may occur. A mixture of coarsen and equiaxed grains was evident in the annealed ULC steel. The morphology of recrystallized structures shows the grains of which average size was in 30 μm. This is in agreement with that recrystallization not only releases much larger amounts of stored energy but new, larger grains are formed by the nucleation of stressed grains and the joining of several grains to form larger ones [13,19,20]. Combination of mechanical properties and microstructure of the steels indicated that the textures made the cold-rolled steel to a low ductility and high strength, or the recrystallized microstructure helped the annealed steels to have a high ductility and low strength.

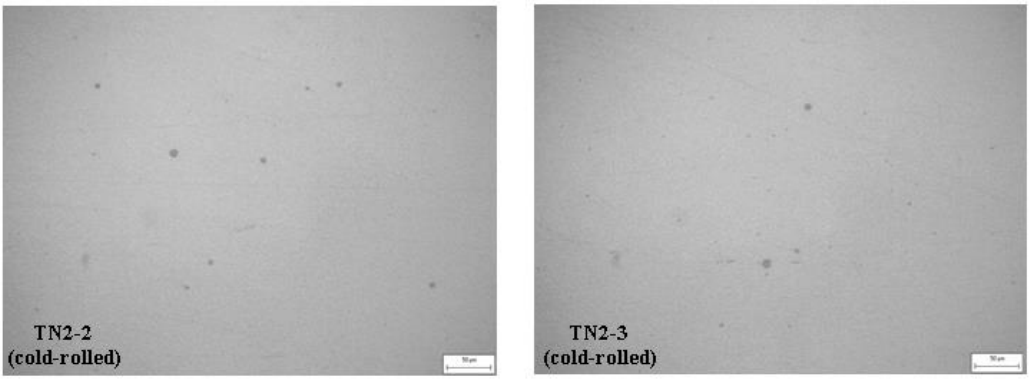

Fig. 3 Optical micrograph of non-metallic inclusions in the ULC steel (TN2-2)

As a general rule, the fewer or less severe the inclusions are, the higher quality steel is. Therefore, analyzing non-metallic inclusions in the present ULC steels have been performed. After proper sample preparation, non-metallic inclusions can be observed directly on the surface of a given steel sample using microscopy. Non-metallic inclusions (in dark spots) in the ULC steels were distributed as **Fig 3**. They could affect. The quantity of the non-metallic inclusion in the ULC steel was calculated based on metallography in assumption of that the quotient of the number of surface particles divided by the area of that surface was equal to the quotient of the number of particles in volume divided by that volume. Relative volume of the inclusions was averagely determined as 0.23 vol. % that was relatively low. This indicated that the inclusions were removed by flotation which enhanced by inductive stirring. T. Lipinski *et al.* have studied on non-metallic inclusions in steel and remarked that their impact depended not only on steel quantity, but also, on their size and distribution in the steel volume; however, they have a significant effect on the performance characteristics, structure, technological and strength parameter of the steel [21]. J. Krawczyk el al. summarized fraction of non-metallic inclusions was in the range 0.21-0.30 vol. % depending on type of the steel [22], meanwhile other research reported that it varied from 0.11-0.24 vol. % in different steels [21].

Induction stirring will always offer the best possibilities for clean steel production. The stirring do not cause a decreasing of the overall volume fraction of the non-metallic inclusions but it changes their shapes, size and distribution. Since inclusions have smaller density than steel, it is reasonable for inclusions sooner or later to float up to the surface. The floatation mechanism is stronger for large inclusions due to Buoyancy forces, so careful examination using SEM

DOI 10.12776/ams.v24i1.1070 p-ISSN 1335-1532
e-ISSN 1338-1156

technique revealed that macro-inclusions (> 15 μm) were hardly to be found in the steel. If existed, they were iron oxide as an example in **Fig 4.** As discussed above, the inductive stirring promoted flotation of the inclusions. Therefore, this iron oxide is speculated to be exogenous and form after finishing vacuum treatment. It may come from the casting mold during pouring the liquid steel. In the practical, large non-metallic inclusions must be as low as possible because they decrease the impact energy of the crack development [21, 22].

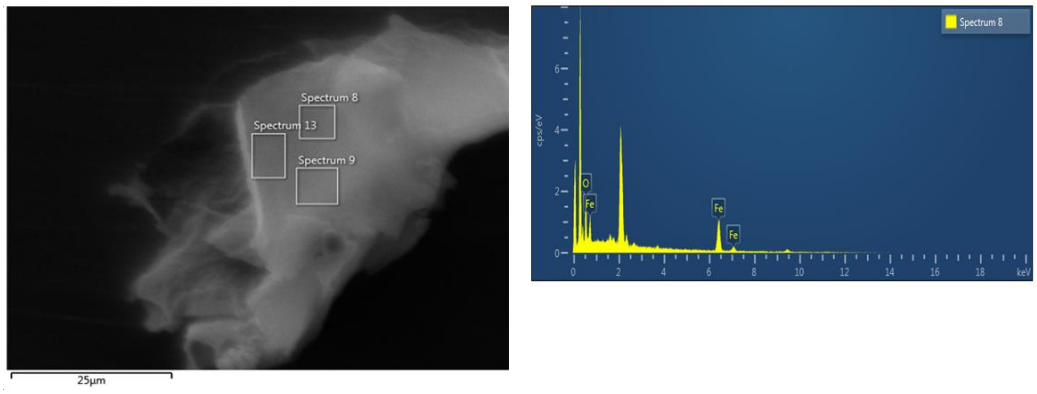

Fig. 4 EDS analysis of non-metallic inclusion in the ULC steel

Microstructure of the ULC anneal steel is also observed by SEM as seen in **Fig. 5,** in which the distribution of ferrite grains size is agreement with optical observation. Since the C contents were ultra-low level, phase structure of the ULC steels must be only ferrite as optical observations. **Fig. 6** shows the XRD patterns of ferrite phase in the cold-rolled and annealed ULC steel (TN2-2). The individual diffracting planes from the body cubic center (bcc) can be clearly identified and labeled in the figure, where it is seen that ferrite peak (110) was prevailed in microstructure of the steels. However, electron backscatter diffraction (EBSD) is considered as a helpful technique to characterize the microstructure, crystal orientation and phase of the steels [23-26]. Further study will be carried out by using this analysis.

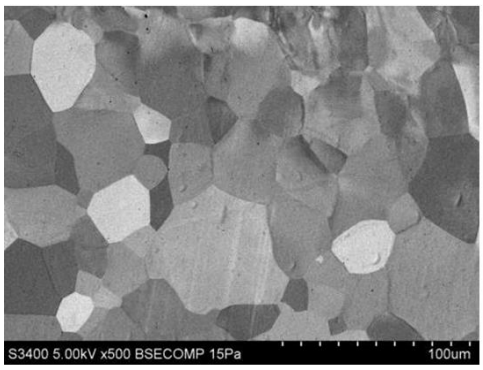

Fig. 5 SEM micrograph of the annealed steel (TN2-2)

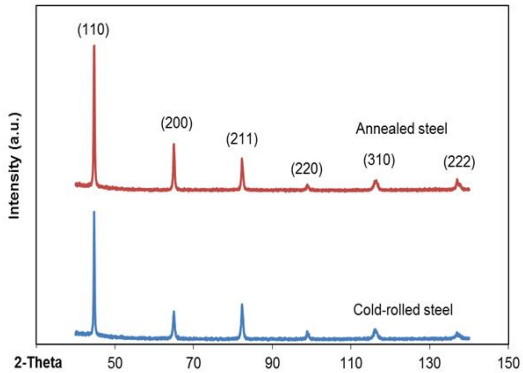

Fig. 6 XRD results of the ULC steels (TN2-2)

DOI 10.12776/ams.v24i1.1070
p-ISSN 1335-1532
e-ISSN 1338-1156

4 Conclusions

Mechanical properties, microstructure and crystallography of the ULC steel after vacuum treatment have been studied. Under the condition of Ar atmosphere of 0.2 atm, it was confirmed experimentally that decarburization of liquid steel has occurred and resulted in ultra-low C content of 36-40 ppm. The efficiency and average rate of decarburization were 82.4-84.2 % and 19 ppm/min, respectively. Relative volume of the inclusions was calculated as relatively low as 0.23 vol. % based on metallography. Microstructural observation of the ULC steel indicated that the textures changed to grains when the steel was annealed at 800°C. The lower YS (199 and 285 MPa) with moderate UTS (309 and 351 MPa) along with high ductility (45.4 and 42.9 %) were obtained for the annealed steel. An increase in the UTS (635 and 777 MPa) with drop in elongation (5.1 and 4.5 %) was achieved due to presence of large residual stress after cold-rolling. It was observed that the (110) ferrite phase, which is the most attractive phase for the application of these steels owing to excellent combination of strength and ductility, was the dominant in these steels despite of that they were in cold-rolled or annealed conditions. EBSD must be used in the further study to investigate the contribution of ferrite grain size, crystalline structure of the present ULC steels.

References

[1] L. Neves, H. P. O. Oliveira, R. Tavares: ISIJ International, Vol. 49, 2009, No. 8, p. 1141-1149, DOI:10.2355/isijinternational.49.1141
[2] J. Liu, R. Harris: ISIJ International, Vol. 39, 1999, No. 1, p. 99-101, DOI:10.2355/isijinternational.39.101
[3] M. Molnar et al.: Acta Metallurgica Slovaca, Vol. 22, 2016, No. 2, p. 95-101, DOI: 10.12776/ams.v22i2.95
[4] W. C. Doo, D. Y. Kim, S. C. Kang, K. W. Yi: Metals and Materials International, Vol. 13, 2007, No. 3, p. 249-255, DOI:10.1007/BF03027809
[5] M. Sano, H. Yetao, M. Kato, S. Sakamoto: ISIJ International, Vol. 34, 1994, No. 8, p. 657-662, DOI:10.2355/isijinternational.34.649
[6] R. Bidulsky, J. Bidulska, M. Actis Grande: High Temperature Materials and Processes, Vol. 32, 2013, No. 5, p. 467-473 DOI: 10.1515/htmp-2012-0174
[7] D. Widlund, D. S. Sarma, P. G. Jonsson: ISIJ International, Vol. 46, 2006, No. 8, p. 1149-1157, DOI:10.2355/isijinternational.46.1149
[8] K. Shoop: The International Journal of Thermal Technology, Nov. 2006, p. 861-867.
[9] M. A. Najafabadi, S. Kanegawa, M. Maeda, M. Sano: ISIJ International, Vol. 36, 1996, No. 10, p. 1229-1236, DOI:10.2355/isijinternational.36.1229
[10] M. A. Makarov, A. A. Aleksandrov, V. Y. Dashevskii: Russian Metallurgy, No. 2, 2007, p. 91-97, DOI: 10.1134/S0036029507020012
[11] A. H. Bui, T. H. Le, B. T. Nguyen: Asean Engineering Journal Part B, Vol. 3, 2014, p. 55-61
[12] J. Galan, L. Samek, P. Verleysen, V. Verbeken, Y. Houbaert: Revista de Metallurgia, Vol. 48, 2012, p. 118-131, DOI: 10.3989/revmetalm.1158
[13] G. Davies: *Materials for automobile bodies*; Elsevier, 2003
[14] A. H. Bui, H. Le: Acta Metallurgica Slovaca, Vol. 22, 2016, No. 1, p. 35-43, DOI: 10.12776/ams.v22i1.690
[15] K. Dehghani, J. J. Jonas: Metallurgical and Materials Transactions A, Vol. 31, 2000, issue 5, p. 1375-1384, DOI: 10.1007/s11661-000-0256-2

[16] M.C. Zhao, K. Yang, Y. Shan: Materials Science and Engineering A335, 2002, issues 1-2, p. 14-20, DOI: 10.1016/S0921-5093(01)01904-9
[17] G. Krauss: Metallurgical and Materials Transactions B34, 2003, issue 6, p. 781-792, DOI: 10.1007/s11663-003-0084-z
[18] T. Ros-Yanez, Y. Houbaert, O. Fischer, J. Schneider: Journal of Materials Processing Technology, Vol. 141, 2003, issue 1, p.132-137, DOI: 10.1016/S0924-0136(03)00247-4
[19] Y. K. Lee, O. Kwon: Journal of Materials Science Letters, Vol. 20, 2001, p. 1319-1321, DOI: 10.1023/A:1010950517953
[20] N. Yoshinaga, H. Inoue, K. Kawasaki, L. Kestens, B. C. De Cooman: Materials Transactions, Vol. 48, 2007, p. 2036-2042, DOI:10.2320/matertrans.MA200704
[21] T. Lipinski, A. Wach: Archives of foundry and engineering, Vol. 14, 2014, No. 4, p. 55-60, DOI: 10.2478/afe-2014-0086
[22] J. Krawczyk, B. Pawlowski: Metallurgy and foundry engineering, Vol. 34, 2008, No. 2, p. 115-124
[23] R. Shukla, S. K. Ghosh, D. Chakrabarti, S. Chatterjee: Metals and Materials International, Vol. 21, No. 1, 2015, p. 85-95, DOI: 10.1007/s12540-015-1010-z
[24] P. Balke, J. Th. M. De Hosson: Scripta Materialia; Vol. 44, 2001, issue 3, p. 461-466, DOI: 10.1016/S1359-6462(00)00632-1
[25] H. R. Wenk, I. Huensche, L. Kestens: Metallurgical and Materials Transactions, Vol. A38, 2007, p. 261-267, DOI: 10.1007/s11661-006-9033-1
[26] R. Bidulsky, J. Bidulska, M. Actis Grande: Metal Science and Heat Treatment, Vol. 58, 2017, No. 11, p. 734-737, DOI: 10.1007/s11041-017-0087-z

Acknowledgements
The authors would like to thank the Ministry of Industry and Trade for financial support (Research contact No. 044-16).